The performance for $B_s^0 \to J/\psi\phi$ and $B^0 \to J/\psi K_S^0$ at LHCb

J. J. van Hunen (for the LHCb collaboration)

NIKHEF, The Netherlands

Received 15 September 2003;
final version 29 September 2003

At LHCb the $B_s^0 \to J/\psi\phi$ decay will be used to determine the B_s^0 mixing phase $\sin\phi_s$ and the decay width difference $\Delta\Gamma_s$, while the $B^0 \to J/\psi K_S^0$ decay will be used to determine the B^0 mixing phase $\sin\phi_d$. A detailed GEANT Monte-Carlo simulation was performed to study the performance at LHCb for these decay channels. The results were used in a 'toy' MC to estimate the sensitivity for $\sin\phi_s$, $\Delta\Gamma_s/\Gamma_s$, and $\sin\phi_d$. The precisions that will be reached after one year of LHCb for $\sin\phi_s$, $\Delta\Gamma_s/\Gamma_s$, and $\sin\phi_d$ are 0.064, 0.018, and 0.022, respectively.

PACS: 62.0
Key words: B-meson, CP-violation, CKM, LHCb

1 Introduction

In this paper a study of the LHCb performance for the decay channels $B_s^0 \to J/\psi\phi$ and $B^0 \to J/\psi K_S^0$ is presented. Also included is an estimate of the precision that can be reached after one year for the B_s^0 mixing phase, $\sin\phi_s$, the B_s^0 decay width difference, $\Delta\Gamma_s$, and the B^0 mixing phase, $\sin\phi_d$. The $B^0 \to J/\psi K_S^0$ decay channel represents a transition to a CP odd eigenstates. The $B_s^0 \to J/\psi\phi$ decay however, represents a decay into a mixture of CP even and odd eigenstate. This mixture arises due to the fact that the ϕ and the J/ψ are both vector mesons and the CP eigenvalue depends on the relative orientation of the polarization vectors of the two vector mesons. Figures 1 and 2 show that the $B_s^0 \to J/\psi\phi$ tree diagram is the SU(3) analogue of the $B^0 \to J/\psi K_S^0$ diagram. In both cases the dominant penguin contribution has a phase that is similar to the tree diagram. The hadronic uncertainties for $B_s^0 \to J/\psi\phi$ are therefore only a few %, while for $B^0 \to J/\psi K_S^0$ they are even smaller than 1%.

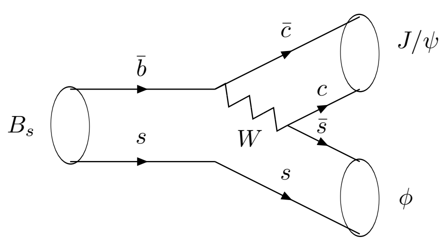

Fig. 1. Tree diagram for $B_s^0 \to J/\psi\phi$.

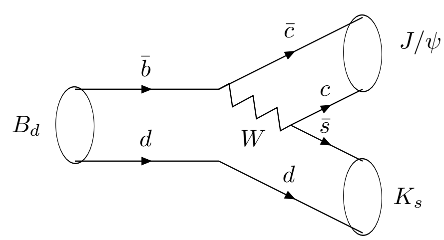

Fig. 2. Tree diagram for $B^0 \to J/\psi K_S^0$.

A $B_s^0(B^0)$-meson can oscillate into a $\overline{B}_s^0(\overline{B}^0)$-meson. Since $B_s^0(B^0)$ as well as

$\overline{\mathrm{B}}_{\mathrm{s}}^0(\overline{\mathrm{B}}^0)$ can decay into $\mathrm{J}/\psi\phi(\mathrm{K}_{\mathrm{S}}^0)$ there is a interference between the decay where the $\mathrm{B}_{\mathrm{s}}^0(\mathrm{B}^0)$ has or has not oscillated. This interference gives a sensitivity to the phase difference between the decay and the oscillation. The phase differences are the $\mathrm{B}_{\mathrm{s}}^0$ and B^0 mixing phases ϕ_{s} and ϕ_{d}, respectively. We define

$$\lambda \equiv \frac{q}{p}\frac{\bar{A}_f}{A_f}, \tag{1}$$

with A_f the instantaneous decay amplitude for a final state f, and p and q the coefficients in the linear combination of B^0 and $\overline{\mathrm{B}}^0$ for the B_s^L and B_s^H mass eigenstates. It then follows that for $\mathrm{B}_{\mathrm{s}}^0 \rightarrow \mathrm{J}/\psi\phi$,

$$\lambda_{\mathrm{B}_{\mathrm{s}}^0\rightarrow \mathrm{J}/\psi\phi} \propto \left(\frac{V_{tb}^* V_{ts}}{V_{tb} V_{ts}^*}\right)\left(\frac{V_{cb} V_{cs}^*}{V_{cb}^* V_{cs}}\right) \rightarrow \Im\lambda_{\mathrm{B}_{\mathrm{s}}^0\rightarrow \mathrm{J}/\psi\phi} = \pm\sin(\phi_s), \tag{2}$$

where the sign in front of $\sin(\phi_s)$ depends on the CP eigenvalue. For $\mathrm{B}^0 \rightarrow \mathrm{J}/\psi\mathrm{K}_{\mathrm{S}}^0$

$$\lambda_{\mathrm{B}^0\rightarrow \mathrm{J}/\psi\mathrm{K}_{\mathrm{S}}^0} \propto \left(\frac{V_{tb}^* V_{td}}{V_{tb} V_{td}^*}\right)\left(\frac{V_{cb} V_{cs}^*}{V_{cb}^* V_{cs}}\right)\left(\frac{V_{cd}^* V_{cs}}{V_{cd} V_{cs}^*}\right) \rightarrow \Im\lambda_{\mathrm{B}^0\rightarrow \mathrm{J}/\psi\mathrm{K}_{\mathrm{S}}^0} = -\sin(\phi_d). \tag{3}$$

The first factor in equations 2 and 3 stands for the $\mathrm{B}_{\mathrm{s}}^0(\mathrm{B}^0)$ oscillation, the second for the tree diagrams shown in figures 1 and 2, while the last term represents the K^0 mixing (only for $\mathrm{B}^0 \rightarrow \mathrm{J}/\psi\mathrm{K}_{\mathrm{S}}^0$). The charge current couplings are represented by V_{ij}.

The time dependent CP asymmetry is defined as

$$\mathcal{A} \equiv \frac{\bar{R}_f(t) - R_f(t)}{\bar{R}_f(t) + R_f(t)} = \frac{(1-|\lambda|^2)\cos(\Delta m t) - 2\Im\lambda\sin(\Delta m t)}{(1+|\lambda|^2)\cosh(\frac{\Delta\Gamma t}{2}) - 2\Re\lambda\sinh(\frac{\Delta\Gamma t}{2})}, \tag{4}$$

with $R_f(t)$ the decay rate for a final state f, Δm the B^0-meson mass difference, and $\Delta\Gamma$ the B^0-meson decay width difference.
It is expected that $\Delta\Gamma_{\mathrm{s}}/\Gamma_{\mathrm{s}}$ is of order 10% [1]. However, $\Delta\Gamma/\Gamma$ can be neglected and in this case the CP asymmetry can be written as

$$\mathcal{A} = \mathcal{A}^{dir}\cos(\Delta m t) + \mathcal{A}^{mix}\sin(\Delta m t). \tag{5}$$

with $\mathcal{A}^{dir} = \frac{(1-|\lambda|^2)}{(1+|\lambda|^2)}$ and $\mathcal{A}^{mix} = \frac{2\Im\lambda}{(1+|\lambda|^2)}$. In the standard model $|\lambda| = 1$, therefore $\mathcal{A}^{dir} = 0$ and $\mathcal{A}^{mix} = \sin(\phi_d)$. Tagging the flavour of the $\mathrm{b}(\bar{\mathrm{b}})$ at production is needed in order to determine the asymmetry from the data. Flavour tagging is done by determining the flavour of the other $\bar{\mathrm{b}}(\mathrm{b})$ that was produced in the pp-interaction from its decay chain (opposite side tagging). For a $\mathrm{B}_{\mathrm{s}}^0(\overline{\mathrm{B}}_{\mathrm{s}}^0)$ it is also possible to determine the flavour of the $\bar{\mathrm{b}}(\mathrm{b})$ directly (same side tagging). If a $\mathrm{B}_{\mathrm{s}}^0(\overline{\mathrm{B}}_{\mathrm{s}}^0)$ is produced there is an additional $\mathrm{s}(\bar{\mathrm{s}})$-quark available in the fragmentation, and in 15% of the cases this results in a kaon close to the $\mathrm{B}_{\mathrm{s}}^0(\overline{\mathrm{B}}_{\mathrm{s}}^0)$. The flavour tagging procedure at LHCb is explained in detail in reference [2].

A measurement of the time dependent asymmetry will provide us with information about $\mathcal{A}^{dir}$ and $\mathcal{A}^{mix}$, and thus with $\sin\phi_s$ and $\sin\phi_d$. Precise measurements exist for $\sin\phi_d$ [3, 4]. For $\sin\phi_s$ this is not the case. The expectation for $\sin\phi_s$ in the CKM picture of CP violation is $\mathcal{O}(0.04)$. If there is physics beyond the standard model this may result in a ϕ_s larger than the expectation. Alternatively, new physics may result in $\mathcal{A}^{dir} \neq 0$ for $B_s^0 \to J/\psi\phi$ or $B^0 \to J/\psi K_S^0$.

1.1 The selection of $B_s^0 \to J/\psi\phi$ and $B^0 \to J/\psi K_S^0$ decays

Proton-proton (pp) interactions are simulated using the PHYTHIA 6.2 [5] event generator, in combination with the QQ [6] program for the decay of particles. The particles are traced through the LHCb apparatus using a GEANT3 [7] detector description. Details about the tuning of PHYTHIA 6.2 and other aspects of the simulation can be found in the LHCb reoptimization TDR [2]. The generated events are analyzed with a selection algorithm that reconstructs the B^0-meson decays. The event selection is optimized to obtain a high reconstruction efficiency for the events of interest (signal), while keeping the background with respect to the signal (B/S) as low as possible. The background level was estimated by analyzing a data sample that contains 10^7 events within 400 mrad that have at least one b or $\bar{b}$-hadron (bb-inclusive data sample). The bb-inclusive events are assumed to be the main source of background in LHCb, since other background events can usually be rejected by making use of the long B^0-meson lifetime and requiring a B^0-decay vertex (secondary vertex) that is well separated from the pp-interaction (primary vertex). This can be accomplished by constraints on the significance of the distance between the primary and secondary vertex (the significance is the ratio of a quantity and the error on this quantity) and the impact parameter (IP) significance of the B^0-meson decay products with respect to the primary vertex.

1.2 Tracking and particle identification

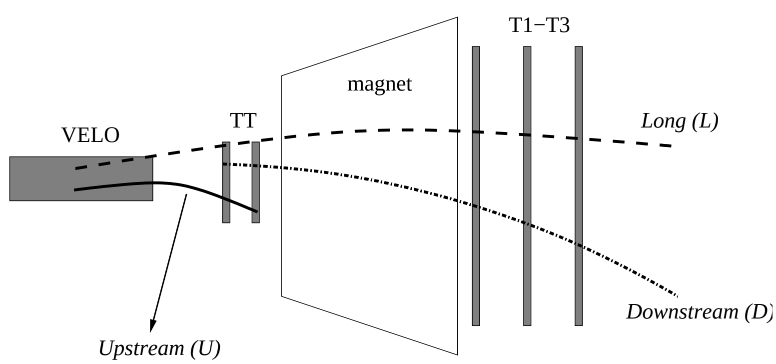

Fig. 3. Schematic view of the LHCb tracker chambers.

The LHCb track reconstruction results in 3 different types of tracks, as shown in figure 3, that can be used to reconstruct the B^0 or B^0_s decays. There are long tracks which have hits in each of the tracking detectors, namely the silicon strip vertex locator (VELO) and trigger tracker (TT), and the T1-T3 stations (a combination of silicon strip and straw tube detectors). Generally only long tracks are used for physics analysis, however in case of the K^0_S-reconstruction use is also made of the upstream and downstream tracks as will be discussed later. For the particle identification (PID) two RICH detectors, a calorimeter system, and a muon detector are used. The tracking and PID are described in detail in the LHCb re-optimization TDR [2].

1.3 Event selection

After the tracking and particle identification the tracks are combined in the event selection to reconstruct J/ψ, ϕ, and K^0_S-mesons. In order to select $J/\psi(\mu\mu)(J/\psi(ee))$ two oppositely charged muons(electrons) are combined to form a common vertex. The invariant mass of the muon combination should be within 50 MeV of the J/ψ mass (3.097 GeV/c^2), while for the electron combination it is required that the invariant mass is between 2.7 and 3.2 GeV/c^2. This mass window is asymmetric since not all Bremsstrahlung photons can be recovered. In order to suppress ghost tracks the electrons should have a transverse momentum, p_T, of at least 0.5 GeV/c, and one electron should have a $p_T > 1.5$ GeV/c. The reconstructed $J/\psi(\mu\mu)$ or J/ψ(ee)-mesons are then combined with a ϕ or K^0_S-meson to reconstruct the $B^0_s \rightarrow J/\psi\phi$ and $B^0 \rightarrow J/\psi K^0_S$ decays.

1.3.1 $B^0_s \rightarrow J/\psi\phi$ decays

The ϕ-meson is reconstructed by combining two oppositely charged kaons and requiring that the invariant mass is within 20 MeV/c^2 of the ϕ mass (1.019 GeV/c^2). Since ϕ-mesons from B^0_s decays have a larger momentum than ϕ-mesons from the primary vertex it is required that the momentum of the ϕ is larger than 12 GeV/c. The ϕ and J/ψ are combined to form the B^0_s. The following constraints are applied:

- The invariant mass of $J/\psi\phi$ combination should be within 50 MeV/$c^2$of the B^0_s mass (5.370 GeV/c^2). In case a J/ψ decays into electrons, it is required that the difference between the invariant mass of the $J/\psi\phi$ and e^+e^- combination is within 50 MeV/$c^2$of the B^0_s and J/ψ mass difference.
- The vertex fit should be good (small χ^2)
- In order to reject the background consisting of J/ψ and ϕ originating from the primary vertex, the significance of the B^0_s decay time is required to be larger than 5. The decay time was determined from a fit with as input the primary and secondary vertex, and the B^0_s momentum.

The resulting mass distribution for the B^0_s is shown in figure 4. The mass resolution is 15 MeV/c^2. The result of applying the same selection on 10^7 bb-inclusive events is shown in figure 5. With a large mass window of ± 600 MeV/c^2 18 events are selected, from which 11 are signal decays (the events in the peak of the distribution) and 7 are background events.

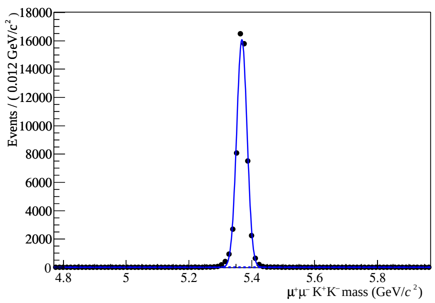

Fig. 4. The B_s^0 mass distribution for $B^0 \to J/\psi(\mu\mu)\phi$ signal events.

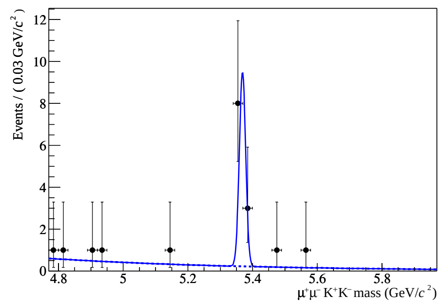

Fig. 5. The B_s^0 mass distribution for $B^0 \to J/\psi(\mu\mu)\phi$ candidates in the bb-inclusive data sample.

1.3.2 $B^0 \to J/\psi K_S^0$ decays

The K_S^0 are selected by combining 2 oppositely charged pions. Also upstream and downstream tracks are included, and from the reconstructed K_S^0-mesons 65% are the result of two downstream tracks (DD), 26% from two long tracks (LL), and 9% from one long and one upstream track (LU). The selection requirements for the K_S^0 and the $J/\psi K_S^0$ combination are slightly different for the different track categories. A complete list of selection cuts is not given here, but can be found in [2]. The resulting mass distributions for $B^0 \to J/\psi(\mu\mu)K_S^0$ are shown in figures 6 (DD category) and 7 (LL category), with core resolutions of 12 MeV/$c^2$and 9 MeV/c^2, respectively. For $B^0 \to J/\psi(ee)K_S^0$ the mass resolutions are shown in figures 8 (DD category) and 9 (LL category), with core resolutions of 20 MeV/c^2 and 17 MeV/c^2, respectively.

1.4 Annual yield and B/S ratio

The annual yield is computed from

$$S = L_{int} \times \sigma_{b\bar{b}} \times 2 \times f_B \times \mathrm{BR_{vis}} \times \epsilon, \tag{6}$$

with L_{int}=2 fb^{-1} the annual integrated luminosity, $\sigma_{\mathrm{b\bar{b}}}$=500 μb the $\mathrm{b\bar{b}}$ production cross section, f_{B} the probability for a $\bar{\mathrm{b}}$ quark to hadronize into B_s^0 or a B^0-meson (10.0% and 39.1%, respectively), $\mathrm{BR_{vis}}$ the product of all branching ratios involved in the decay, and ϵ the efficiency for reconstructing signal events (including the effect of the limited geometrical acceptance, the cluster and track finding efficiency, the efficiency of the selection cuts, trigger efficiency, etc.). The factor 2 takes the production of $\bar{\mathrm{b}}$ and b into account.

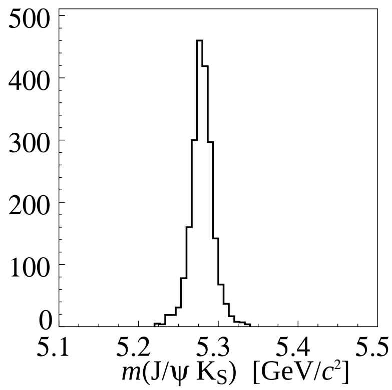

Fig. 6. The B_d^0 mass $B^0 \rightarrow J/\psi(\mu\mu)K_S^0$ decays, where the K_S^0 is reconstructed with two downstream tracks.

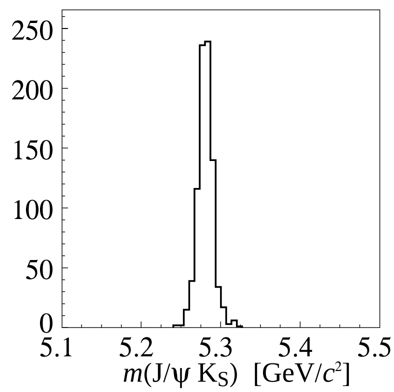

Fig. 7. The B_d^0 mass $B^0 \rightarrow J/\psi(\mu\mu)K_S^0$ decays, where the K_S^0 is reconstructed with two long tracks.

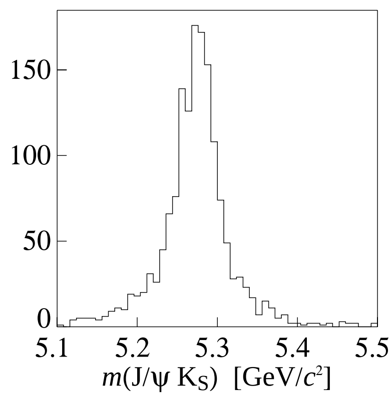

Fig. 8. The B_d^0 mass distribution for $B^0 \rightarrow J/\psi(ee)K_S^0$ decays, where the K_S^0 is reconstructed with two downstream tracks.

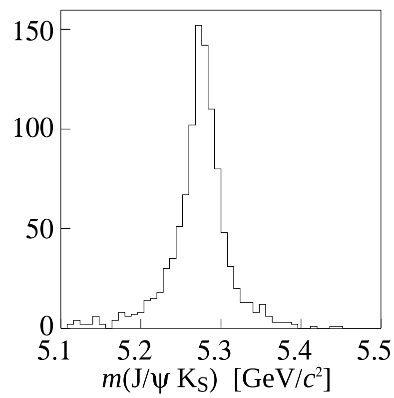

Fig. 9. The B_d^0 mass distribution for $B^0 \rightarrow J/\psi(ee)K_S^0$ decays, where the K_S^0 is reconstructed with two long tracks.

The annual yields are shown together with the B/S ratios and the tagging performance (the tagging efficiency $\epsilon_{tagging}$, and the wrong tag fraction w) in table 1.

2 Sensitivity for $\sin\phi_s$, $\Delta\Gamma_s/\Gamma_s$, and $\sin\phi_d$.

To estimate the statistical precision on $\sin\phi_s$, $\Delta\Gamma_s/\Gamma_s$, and $\sin\phi_d$ after one year of LHCb, toy MC studies have been performed. In these toy MC's the results of the full GEANT simulation, such as the event yields, the B/S ratios, the decay time resolutions, and the tagging performance, are used. Events are generated for

Table 1. Annual yield, the B/S ratio and the tagging performance.

decay	BR_{vis} 10^{-6}	ϵ %	Annual yield 10^3	B/S	w %	$\epsilon_{tagging}$ %
$B_s^0 \to J/\psi(\mu\mu)\phi$	31	1.672	100	<0.3	33.4±0.4	50.4±0.3
$B_s^0 \to J/\psi(ee)\phi$	31	0.315	20	0.7±0.2	-	-
$B^0 \to J/\psi(\mu\mu)K_S^0$	19.8	1.39	216	0.80±0.10	36.7±1.9	45.1±1.3
$B^0 \to J/\psi(ee)K_S^0$	20.0	0.164	25.6	0.98±0.21	34.3±0.7	41.9±0.5

different settings of the CP parameters, such as sinϕ_s, $\Delta\Gamma_s/\Gamma_s$, the fraction of CP odd final states in $B_s^0 \to J/\psi\phi$, R_{odd}, and Δm_s. For each setting of these parameters the time dependent CP asymmetry, equation 5 for $B^0 \to J/\psi K_S^0$ and equation 4 for $B_s^0 \to J/\psi\phi$, is fitted with an unbinned likelihood to extract the values for sinϕ_s, $\Delta\Gamma_s/\Gamma_s$, and sinϕ_d.

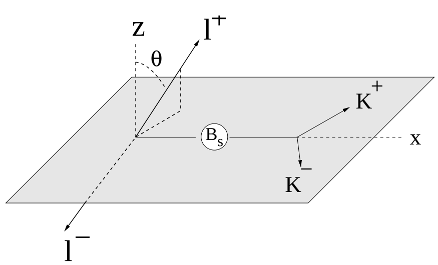

Fig. 10. Definition of the transversity angle θ. In the rest-frame of the J/ψ the transversity angle is the angle between the z-axis and the positive lepton (l^+). The z-axis is perpendicular to the plain made up by the two kaons from the ϕ.

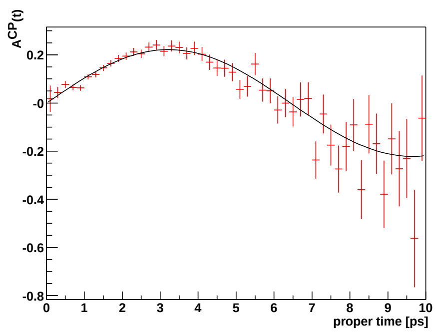

Fig. 11. The background subtracted asymmetry $\mathcal{A}$ for one year of $B^0 \to J/\psi K_S^0$ data. The curve represents the fit with the expression for the asymmetry, equation 5.

Due to the mixture of CP-even and CP-odd final states in the $B_s^0 \to J/\psi\phi$ decay it is needed to perform the unbinned likelihood fit to the decay time distribution as well as the transversity angle distribution. The transversity angle, defined in figure 10, allows us to disentangle the CP odd and CP even contribution to the asymmetry. The results of the likelihood maximization for sinϕ_s and $\Delta\Gamma_s/\Gamma_s$ are shown in table 2 For the $B^0 \to J/\psi K_S^0$ data an unbinned likelihood fit has been performed with the function $(1-2w) \times \mathcal{A}$. The result is shown in figure 11. The free parameters were $\Im\lambda$ and $|\lambda|$, while w was fixed to 34.3%. An uncertainty on w - as obtained from the analysis of the control channel $B^0 \to J/\psi K^{*0}$ - was taken into account in the fit. The statistical uncertainty on $\Im\lambda$ and $|\lambda|$ from the fit are 0.022 and 0.023, respectively.

Table 2. Statistical precision on $\sin\phi_s$ and $\Delta\Gamma_s/\Gamma_s$ after one year of data taking. Unless otherwise specified, $\Delta m_s = 20\,\text{ps}^{-1}$, $\Delta\Gamma_s/\Gamma_s = 0.1$, $\sin\phi_s = -0.04$, $R_T = 0.2$.

Δm_s in ps^{-1}	15	20	25	30
$\sigma(\sin\phi_s)$	0.0597	0.064	0.075	0.088
$\sigma(\Delta\Gamma_s/\Gamma_s)$	0.018	0.018	0.018	0.018

$\Delta\Gamma_s/\Gamma_s$	0	0.1	0.2
$\sigma(\sin\phi_s)$	0.059	0.064	0.070
$\sigma(\Delta\Gamma_s/\Gamma_s)$	0.015	0.018	0.019

$\sin\phi_s$	0	−0.04	−0.1	−0.2
$\sigma(\sin\phi_s)$	0.064	0.064	0.064	0.066
$\sigma(\Delta\Gamma_s/\Gamma_s)$	0.018	0.018	0.018	0.018

R_{odd}	0.1	0.2	0.3
$\sigma(\sin\phi_s)$	0.050	0.064	0.084
$\sigma(\Delta\Gamma_s/\Gamma_s)$	0.015	0.018	0.019

3 Discussion and Conclusion

A full GEANT MC simulation of the LHCb detector was used in combination with toy MC programs to estimate the precision on $\sin\phi_s$, $\Delta\Gamma_s/\Gamma_s$, and $\sin\phi_d$ after one year of LHCb data taking. The precisions were found to be 0.064, 0.018, and 0.022 respectively. The existence of physics beyond the standard model could become clear from a deviation from $\sin\phi_s$ with respect to the standard model value of 0.04, or from a sizable contribution of $\mathcal{A}_{dir}$ to the time dependent asymmetry in $B^0 \to J/\psi K^0_S$ and $B^0_s \to J/\psi\phi$ decays.

References

[1] M. Beneke and A. Lenz, J.Phys. G27 (2001) 1219

[2] LHCb Reoptimized Detector Design and Performance, CERN/LHCC 2003-030, LHCb TDR 9, ISBN 92-9083-209-6.

[3] BABAR Collaboration, B. Aubert et al., Phys. Rev. Lett .89, 201802 (2002).

[4] Belle Collaboration, K. Abe et al., Phys. Rev. D 87, 071102(R) (2002).

[5] T. Sjöstrand et al., Computer Physics Commun. 135 (2001) 238.

[6] QQ Program, http://www.lns.cornell.edu/public/CLEO/soft/QQ.

[7] GEANT Detector description and simulation tool, CERN Program Library, long write-up W5013 (1994)